Clin Transl Imaging (2016) 4:297–306
DOI 10.1007/s40336-016-0186-7

REVIEW ARTICLE

The role of iodine-124 positron emission tomography in molecular imaging

Sonia Mahajan[1] · **Chaitanya R. Divgi**[1]

Received: 29 March 2016 / Accepted: 17 May 2016 / Published online: 8 June 2016

Abstract Radioactive iodine has been, in various forms, the mainstay of Nuclear Medicine. Iodine-123 is the most widely used iodine isotope for single photon imaging. Iodine-125 continues to be used in diverse applications from in vitro radioassay to in vivo estimation of various pathophysiologic correlates. Iodine-131 (^{131}I), useful for imaging as well as therapy, has contributed more than any other radionuclide to the growth and sustenance of Nuclear Medicine. Positron emission tomography (PET) is an indispensable tool in current clinical practice, spurred by the rapid and increasing availability of radiopharmaceuticals for in vivo imaging. Most clinical PET imaging utilizes fluorine-18; there is a need for positron emitters with longer half-lives, suitable for imaging larger molecules of interest. Iodine-124 (^{124}I) has approximately 23 % positron emission; its 4-day half-life lends itself to sequential imaging, and its dosimetry is comparable to iodine-131. Iodine can be easily attached to a variety of molecules without alteration of physico-chemical or biologic properties. PET with ^{124}I-labeled molecules enables longitudinal in vivo assessment of their distribution; such pharmacokinetic and biodistribution information has considerable utility in oncologic and non-oncologic applications. We will provide a clinical perspective on the physical and chemical characteristics of ^{124}I, as the iodide, as well as radiolabeled to a wide variety of molecules of interest. Radioiodination is accomplished based on the chemical and biologic nature of the ligand to be studied, and issues of relevance will be highlighted. We will conclude by describing the current and potential future clinical applications of ^{124}I-based tracers used for molecular imaging in diagnosis and therapy.

Keywords ^{124}I · Radioiodine · Radiopharmaceuticals · Molecular imaging · Biodistribution, quantification

✉ Chaitanya R. Divgi
divgic@gmail.com

Sonia Mahajan
soniamahajandinesh@gmail.com

[1] Department of Radiology, Columbia University Medical Center, 622 W 168 Street, New York, NY 10032, USA

Iodine and its isotopes

Iodine is an important trace element necessary for proper function and development of human body. As the iodide, it forms an essential component of thyroid hormones which are responsible for regulation of various metabolic processes in the body. Iodine (atomic number 53) has approximately 37 isotopes that can be produced in a nuclear reactor or cyclotron. Those isotopes that are used in the diagnosis and therapy of medical disorders will be illustrated here with reference to ^{124}I, the isotope of review.

The thyroid has the ability to trap iodine via integral membrane proteins called sodium-iodide symporters (NIS) residing in the epithelial basolateral membrane of thyroid follicular cells. The trapped iodine is integral to thyroid hormone synthesis. Functional characteristics of the thyroid in health and disease may thus be assessed by imaging and measuring radioiodine thyroid uptake. Such measures, in addition to providing pathophysiologic information, optimize treatment with ^{131}I. Iodine is absorbed as the iodide through ingestion, inhalation, puncture, wound and skin contamination. It is concentrated in the salivary glands, thyroid and gastric mucosa, and the choroid plexus in the brain. The critical organ in humans is the thyroid and

the predominant route of iodide excretion is through the urine, with variable fecal excretion. The long biological half-life of iodide is 120–138 days primarily due to incorporation into thyroid hormone and precursor proteins. Iodide is not retained intracellularly, and thus clears rapidly from non-target tissues.

Iodine-123 and -131, with half-lives (T1/2) of 13.3 h and 8.02 days respectively, have been increasingly used for measuring radioiodine uptake, and imaging its in vivo distribution at multiple times after ingestion. Iodine-123 is widely used in delineation of thyroid functional status and assessment of thyroid nodules. Its principal photon emission of 159 keV is ideally suited to successful single photon imaging on modern gamma cameras optimized for imaging the 140 keV photon of technetium-99 m (99mTc), the most widely used single photon radionuclide.

Iodine-131 is widely used in the diagnosis and therapy of thyroid disorders. Widely available and relatively inexpensive, with abundant principal photon emission of 364 keV and long physical *T*1/2 of 8.02 days, it may be used to image bio-distribution and dosimetry for several days after ingestion. These images enable decisions regarding therapy with ^{131}I; the nuclide emits beta rays (average β-minus 606 keV), enabling successful therapy in hyperthyroidism as well as thyroid cancer. It may be sometimes necessary to calculate ^{131}I absorbed doses for vital organs like bone marrow, particularly before treatment with large amounts of ^{131}I in thyroid cancer.

Iodine-125 in its unsealed form is mainly used for in vitro assays. Its long half-life of 60 days and low energy gamma photon emission (27, 35 keV) makes it unsuitable for patient imaging (though suitable as a sealed source for high dose brachytherapy).

Iodine-124, with a T1/2 of 4.2 days, is a positron emitting isotope of iodine. It may be used for PET imaging in humans as the iodide, as well as attached to a broad range of molecules of varying size. PET permits in vivo quantification of bio-distribution and dosimetry. PET with ^{124}I has thus found several oncologic and non-oncologic applications. This clinically oriented review will include a brief description of its physicochemical properties including reference to its use as a radiolabel, followed by a discussion of its current applications in clinical and research molecular imaging.

A thorough literature search was carried out in two phases. In the first phase, literature search of Medline and Google Scholar databases yielded approximately 950 studies using the keywords Iodine124, ^{124}I with Boolean operator OR. In the second phase, the potential relevance was examined and the number was reduced by excluding the studies not associated directly with properties and role of ^{124}I in imaging and quantitation.

Physico-chemical properties of ^{124}I

Physical characteristics

Iodine-124 decays, by dual energy positron emission (1532 keV (11 %) and 2135 keV (11 %)) and electron capture with gamma emissions of 511 keV (46 %), 603 keV (61 %) and 1691 keV (11 %) [1]. About a quarter of all decay events thus result in positron emission, unlike 18F, where positron emission occurs in >96 % of decay events. The high positron energy makes it travel a longer distance (than 18F) before it annihilates with an electron, which can give result in a falsely identified line of response (LOR) [2]. The single photon emissions also negatively impact the resolution, and signal to noise ratio of images. While initial PET imaging could be satisfactorily conducted with septal collimation, current 3D PET/CT devices implement suitable reconstruction algorithms [2, 3]. Spatial resolution, count rate performance, sensitivity and scatter fraction, and other measures have now been found to be quite satisfactory for 3D reconstruction methods [4]. Radiation dose to human subjects is comparable to ^{131}I, though higher than 18F [4].

Production

Tellurium, in its natural state, is composed of many isotopes and can give rise to multiple radioiodine daughters. Iodine-124 is produced by bombardment of an enriched tellurium-124 (^{124}Te) solid target in a cyclotron. ^{124}Te enrichment is expensive, and this is invariably reflected in the cost of ^{124}I. The method initially used for production of ^{124}I involved enriched ^{124}Te in a ^{124}Te(d,2n)^{124}I reaction. However, this has largely been replaced by the ^{124}Te(p,n)^{124}I, which has the advantages of being produced by proton bombardment with incident beam energy of 11 or 14 MeV (based on the target composition), a feasible and indeed preferred method in most 16-18 MeV medical cyclotrons [5]. This results in a good target yield with high radionuclidic purity and low quantity of impurities like 123I and ^{125}I [6].

Multiple factors like target composition, thermal stability of the irradiated sample and selection of target support can influence the production of ^{124}I. The target material is usually tellurium oxide (TeO_2) with 5 % by mass aluminium hydroxide (Al_2O_3) added to improve heat exchange and prevent vaporization of ^{124}I [7, 8]. Adequate thermal control is crucial to high current target irradiations, and is achieved by cooling the back of the target support plate with water, and the front with helium [5].

Recently, a robotic, fully automated system for large scale production of ^{124}I has been developed in Japan,

which uses a capsulated target and gives good yield. The capsule consists of three pieces of gold (99.99 %), which have shown best chemical resistance against TeO_2 under high temperatures. Enriched TeO_2 with alumina is used as target material and the calculated proton energy on the target surface is 11.6 MeV for the $^{124}Te(p,n)^{124}I$ reaction. The capsulated target can be reused repeatedly and requires no special processing, adding to the economic efficiency of the procedure [9]. Other target materials have also been investigated for production, particularly antimony (Sb), in a $^{123}Sb(\alpha,3n)^{124}I$ reaction, yielding sufficient amount of ^{124}I with relatively low level of ^{125}I and 126I impurities [10, 11]. However, the reaction requires an alpha particle beam in a cyclotron of intermediate energy.

The ^{124}I is extracted from the oxide target by dry distillation in a quartz capillary tube with gas flow to remove traces of TeO_2, trap radioiodine and retain the target material on the target plate. To increase trapping efficiency, the tubes are usually primed with sodium hydroxide (NaOH). ^{124}I settled on the walls of the tube can be recovered by washing with a weak buffer solution while recovery of target material ensures its reuse and economic sustainability [5, 6].

Attachment of ^{124}I to molecules of interest

^{124}I, like all iodine isotopes, is a volatile halide, and care must be taken to avoid contamination including particularly inhalation. Since it is a large atom, it can modify the in vitro and in vivo pharmacological properties of a molecule after attachment. To circumvent the latter issue, the iodine atom is introduced in a position as far as possible from the pharmacophore. There are both direct and indirect methods of radioiodination, accomplished by either electrophilic or nucleophilic substitution reactions [5].

Direct iodination with iodide as the nucleophile in an oxidation state of -1 can be carried out in a simple nucleophilic substitution reaction. This can be used in the radioiodination of both aliphatic and aromatic compounds; however, it proceeds slowly with aromatic compounds. To accelerate the process, metal-assisted reactions can be useful, like copper (I) and copper (II) assisted radio-iodination [12].

Iodine can be easily oxidized by a variety of oxidants. Chloramine-T (used in some mouthwash) is efficient, and its fairly strong oxidizing properties may be mitigated by immobilization onto polystyrene beads (Iodobeads). Iodogen, peracetic acid, hydrogen peroxides and other mild oxidizing agents, and enzymes like lactoperoxidase, are preferred for sensitive substrates [13]. Oxidation reactions help form a reactive electrophilic species with an oxidation state of +1. This species can conveniently substitute an activated proton from the aromatic ring of tyrosine in the ortho position to a phenol group, useful in labelling aromatic compounds. A disadvantage to this method is the lack of regioselectivity, i.e., formation of the chemical bond with preference for a particular direction of bond making or breaking over all other possible directions, with simultaneous production of numerous isomers that are difficult to separate. However, due to its intrinsic simplicity, electrophilic substitution remains the most commonly employed method for radio-iodination [14]. Metal cations and strong acids can be harsh to organic materials, while N-halosuccinimides such as N-bromosuccinimide, are rarely used due to the possibility of chlorination, oxidation side reactions and need for aggressive solvent systems [15].

The carbon-iodine bond in aliphatic compounds is not very stable and may result in deiodination in vivo, leading to accumulation in salivary glands, thyroid and stomach (consequently, clinical use of radioiodine for other than thyroid disorders includes administration of a large amount of stable iodide to block these normal uptake sites.) This has led to the exploration of more stable methods of attachment.

Indirect methods of electrophilic radio-iodination include demetallation using organometallic compounds, which have the advantages of using very little precursor, and regioselective labeling of non-carrier added radiopharmaceuticals with a high yield under relatively mild conditions. Compounds like organo-boranes, silicon, germanium, tin, organo-mercury and organo-thallium have been used. Destannylation appears to be the most preferred reaction due to highly selective cleavage of the weak sp^2 tin-carbon bond. However, tin compounds are toxic and the organo-tin reagents used in synthesis need to be removed via time-consuming purification methods, reducing radiochemical yield. To circumvent this problem, Hunter et al. developed an insoluble polystyrene resin with a reactive dialkyl tin moiety that can be functionalized to a variety of polymer-supported arylstannanes [16]. This approach, commercialized as Ultratrace™ Resin, avoids toxic impurities observed in solution by tethering the reactive arylstannane to the solid support.

Indirect protein radioiodination has been carried out with a range of prosthetic groups. They differ vastly with respect to overall synthesis time, radiochemical yield, efficiency of conjugation to the biomolecule, chemoselectivity of conjugation step and influence of the group on ligand pharmacokinetics. ^{124}I-SHPP (*N*-succinimidyl 3-(4-hydroxy-5-iodophenyl) propionate) or Bolton-Hunter reagent has been used to indirectly label the VEGF antibody for imaging tumor angiogenesis, and an anti-HER2 antigen-binding protein for PET imaging of HER2-expressing tumors (Glaser et al., Chacko et al.). ^{124}I-SHPP has a tendency to undergo enzymatic de-iodination in vivo and in order to achieve radiolabel stability, a variety of

radioiodinated carboxylic acid esters have been developed for conjugation to proteins [17]. Other prosthetic groups, notably *N*-succinimidyl-3 or 4-^{124}I-iodobenzoate (3- or 4-[^{124}I] SIB) have been successfully conjugated to proteins.

Applications

^{124}I in thyroid disease

In the characterization of benign thyroid disorders, ^{124}I may prove beneficial over planar scintigraphy/SPECT imaging using 99mTc-pertechnetate or ^{123}I. It has the advantage of higher resolution images, computed tomography and superior delineation of nodules. In a study conducted by Darr et al., low activity ^{124}I-PET/low dose CT detected significantly more hot and cold nodules than 99mTc planar/SPECT imaging [18]. More patients with retrosternal thyroid tissue were identified, demonstrating the potential of ^{124}I PET to provide superior imaging of benign thyroid disease. The implications of better detection of discernible nodules on management is yet to be analyzed.

^{124}I-PET has proven useful in staging of recurrent and residual disease in thyroid malignancy [19–21]. Phan et al. showed in their study that ^{124}I scans pre-therapy detected more lesions than ^{131}I imaging, with results comparable to the post-^{131}I therapy scan. Only 3 of 11 patients with positive ^{124}I scans had positive pre-therapy ^{131}I scans, with 2 of 5 patients with negative ^{131}I scans showing positive lesions on ^{124}I PET [22]. A comparison between ^{124}I and 18F-Fludeoxyglucose (18F-FDG) PET in 21 patients with differentiated thyroid cancer (DTC) reported sensitivities of 80 % and 70 %, respectively [23]. Capoccetti et al. [24] reported matching ^{124}I PET and ^{131}I WBS results in 58 of 67 patients with additional findings in 10. Similar results were seen in other studies as well.

The utilization of ^{131}I-therapy for benign and malignant thyroid disease is already well established. ^{131}I has a principal gamma emission of 364 keV that is considerably higher than the ideal for imaging with gamma cameras. Several groups have demonstrated that ^{124}I image acquisition in 3D mode is feasible even in the presence of large amounts of ^{131}I on a standard clinical PET scanner [25]. Even with low amounts of ^{124}I ($\sim$74 MBq), a time of flight PET/CT scanner showed comparable lesion detectability as ^{131}I WBS for small spheres less than equal to 10 mm as reported by Beijst et al. using NEMA phantoms [26].

Dosimetry: Simultaneous administration of ^{124}I enables in vivo determination of bio-distribution and dosimetry of ^{131}I. It helps to measure (average) absorbed doses of ^{131}I to organs of interest, enabling quantitative dose–response studies, dose planning before therapy, dose evaluation during therapy and further investigations of the "stunning" phenomenon [27–31]. On the basis of a theoretical dosimetry based model using ^{124}I, Jentzen et al., showed that the lowest effective therapy activity required for thyroid remnant ablation in low risk differentiated thyroid cancer appears to be approximately 2.2 GBq [32]. In a study by Hartung-Knemeyer et al. [33], 198 patients with DTC had undergone a pre-therapeutic blood dosimetry using ^{124}I and values were compared with blood dose administered post ^{131}I therapy. There was a clear correlation between cytopenia and predicted blood doses for both white cells and platelets. Ho et al. used ^{124}I for dosimetry before administering radioiodine-131 therapy in patients treated with selumetenib (MEK1 and MEK2 inhibitor). Selumetenib increased the uptake of ^{124}I in 12 of 20 patients, and effectiveness was found to be greater in patients with RAS-mutant disease [34]. The utility of pretherapeutic ^{124}I PET/CT dosimetry as a prognostic tool and in assessment of dose–response relationship was recently illustrated by Wierts et al. [35]. All lesions were accurately identified and the threshold absorbed dose value calculated for remnants and metastases to predict the achievement of complete response was calculated to be 90 Gy and 40 Gy respectively. In contrast, a multicenter diagnostic cohort study (THYROPET) by Kist et al. [36], showed a high false negative rate of ^{124}I PET/CT in patients with biochemical evidence of recurrent thyroid cancer and negative ultrasound. However, the number of patients included in the study were small ($n = 17$) as it was terminated preliminarily, after three patients had a negative ^{124}I PET/CT and a positive post therapy ^{131}I. Another retrospective study by Khorjekar et al. [37] showed a low predictive value of a negative ^{124}I PET scan in patients with elevated serum Tg levels and negative diagnostic ^{131}I scan. Further validation studies with higher sample size may be needed to determine the value of pretherapeutic ^{124}I PET scans.

^{124}I labelled biomacromolecules

There is increasing interest in radiolabelling large biomolecules (oligonucleotides, oligosaccharides, peptides and proteins) and macromolecules especially monoclonal antibodies for applications in diagnosis and treatment of diseases.

Girentuximab (cG250) is a chimeric antibody that binds to carbonic anhydrase IX, expressed on more than 95 % of clear cell renal cell cancer (ccRCC). ^{124}I-girentuximab PET/CT was demonstrated to be useful in identifying the ccRCC phenotype with high accuracy, in an initial single center verification trial with 25 patients, validated subsequently in a multi-center study with 226 patients [38, 39]. It represents the first molecular imaging modality that identifies an immunohistologically specific prognostic marker for a human solid tumor.

Pryma et al. further demonstrated a linear relationship between in vivo estimates of antibody uptake measured by ^{124}I PET/CT with ex vivo biopsy measurements of radioactivity, confirming the ability of PET/CT with ^{124}I to provide quantitative estimates of radioactivity in normal organs and tumors [40].

^{124}I-huA33—Antibody huA33 recognizes the A33 antigen, present in more than 95 % of colorectal cancers and in normal bowel. ^{124}I-huA33 PET/CT has been utilized at Memorial Sloan-Kettering Cancer Center to demonstrate targeting of the antibody to colorectal metastases, confirming previous work done by the group to establish the utility of this antibody for radioimmunotargeting [41, 42].

Schwartz et al. demonstrated that red marrow radiation absorbed dose could be identified in both the above instances, with the potential to estimate the optimal therapeutic dose for radioimmunotherapy [43].

Several other antibodies have been studied in murine models, including ^{124}I-VEGF MAB HUMV833,which was evaluated in a human tumor xenograft model [44], and another antibody targeting neo-vasculature, which employed a murine model with murine VEGFr-positive cells [45].

^{124}I labelled mIBG

Meta-iodobenzylguanidine is a structural analogue of guanethidine. It shows energy dependent uptake mediated by nor-epinephrine transporter in cells rich in sympathetic neurons. It is used both as a diagnostic and therapeutic tool in neuroendocrine tumors and neuroblastoma [46–48].

Patients undergo ^{123}I-mIBG or low dose ^{131}I-mIBG single photon imaging to identify sites of disease (and suitability for ^{131}I-mIBG therapy) predict the organ and whole body dose, which can guide in deciding on a safe therapeutic dose for each patient. Moreover, quantification of single photons in vivo can be fraught. ^{123}I-mIBG has been found to be inferior to 18F-FDG in depicting lesions in stage I and II neuroblastoma [49]. Images are obtained the day after injection; later imaging is difficult given the 13-hour half-life of ^{123}I.

^{124}I-mIBG permits better identification of disease as well as more accurate quantification of radiation dose to normal and pathological organs, with the potential for more precise I131-mIBG therapy. Improvement in sensitivity, lesion detection, increased precision to count individual lesions and better characterization of skull lesions are incremental benefits. Accurate determination of semi-quantitative TMRR (Total ^{123}I-MIBG retention ratio), MIBG/Curie score and SIOPEN (International Society of Pediatric Oncology Europe Neuroblastoma Group) score during scan interpretation improves extent of disease evaluation and may help in deciding the appropriate next step in management i.e., choosing between medical and surgical treatment [50–53]. The scoring, typically done using ^{123}I-mIBG, will likely be improved with ^{124}I-mIBG PET; the longer half-life of ^{124}I also enables delayed images up to a week after administration.

Preliminary experience in two pediatric patients with an IV dose of 50 MBq and image acquisition done at 24 and 48 h showed promise [53]. Improved characteristics of current PET/CT scanners allow decreasing administered amount of radioactivity while maintaining adequate image quality [54], though it must be noted that radiation exposure is a secondary concern in these children with life-threatening disease and considerable mutagenic therapy. Further investigational studies are warranted to validate and standardize the use of ^{124}I-mIBG in patients with neuroblastoma.

Patient specific dosimetry for ^{131}I-mIBG using pretherapy ^{124}I-mIBG and Monte Carlo dosimetry has recently been used for better treatment planning. This method estimated dose to normal organs and tumors with more realistic simulation geometry [55]. Organ-absorbed doses for the salivary glands, heart wall and liver were determined to be 98.0 Gy, 36.5 Gy, and 34.3 Gy, respectively, whereas tumor-absorbed dose range was 143.9–1641.3 Gy.

Hypoxia imaging

Tumor hypoxia is associated with aggressive tumor phenotypes, and increased resistance to chemotherapy/radiotherapy; it is an independent prognostic factor of clinical outcome. New therapies like hypoxia-activated prodrugs, and hypoxia triggered gene therapy are being developed and the need to assess tumor hypoxia is necessary to select patients who will benefit with this therapy [56]. Many members of the 2-nitroimidazole family have been investigated, including ^{124}I- iodoazomycinarabinofuranoside (IAZA) and ^{124}I-IAZGP. None has been shown to be superior to 18F-labeled compounds [57, 58]. Reischl et al. performed a study to compare ^{124}I-IAZA, 18F-FAZA and 18F-MISO in visualization of tumor hypoxia in a mouse model of human cancer using microPET and showed that 18F-FAZA has superior biokinetics compared to the others; imaging at later time points was of no advantage for ^{124}I-IAZA as the absolute whole body radioactivity was then very low [59].

Nanoparticles

Nanoparticles coated with appropriate ligands can be targeted to specific cells. Incorporating ^{124}I to the structure of nanoparticles retains their bio-functionality and enables PET imaging [60]. Animal studies using ^{124}I-labelled nanopolymers targeted to specific endothelial determinants

aid in optimization of targeted drug delivery, and nanophosphors tagged with radiolabelled (^{124}I) RGD for tumor imaging, have shown promising results [61, 62].

Other compounds of interest

^{124}I-Beta-CIT (^{124}I-2beta-carboxymethoxy-3beta-(4-iodophenyl)tropane) is a cocaine analog that binds to dopamine transporter and has been used to image the sub-thalamic nuclei in drug abuse and Parkinson's disease. In a normal brain, there is high tracer accumulation in striatum and much lower in the thalamus, neocortex and cerebellum. ^{124}I potentially provides quantification, with its long half-life also permitting delayed imaging [12]. ^{124}I-Epidepride for extended imaging of dopamine D2/3 receptors may have applications in imaging of receptors in brain and pancreatic islet cells [63]. ^{124}-I labelled to a small molecule, *MIP-1095,* that targets prostate specific membrane antigen was used for dosimetry as a guide to therapy with the 131-I labelled molecule [64].

The suitable half-life, quantifiable and relatively abundant positron emission, and well characterized chemistry, have led to a plethora of ^{124}I labeled compounds being developed; most have currently not gone beyond rodent imaging studies. ^{124}I-labeled CDK4/6 inhibitors [65], 1-(2-deoxy-beta-D-ribofuranosyl)-2,4-difluoro-5-iodobenzene (^{124}I-dRFIB) [66] and ^{124}I-deoxyuridine (^{124}I-IUdR) have been developed for use in imaging cell proliferation. ^{124}I-IUdR) has been used to measure cell proliferation in vivo in non small cell lung cancer [67] and glioma [68]. ^{124}I-labeled-hypericin for imaging protein-kinase C, 2′-fluoro-2′-deoxy-1β-D-arabinofuranosyl-5-[^{124}I]iodouracil (^{124}I-FIAU) for imaging herpes virus thymidine kinase [69], (E)-But-2-enedioic acid [4-(3-[(^{124})I]iodoanilino)-quinazolin-6-yl]-amide-(3-morpholin-4-yl-propyl)-amide (^{124}I-morpholino-IPQA) for imaging EGFR kinase activity [70], ^{124}I-labeled-6-anilino-quianilino-quinazoline for imaging EGFR Inhibitor, ^{124}I-labeled Annexin V and MBP Annexin V for imaging of apoptosis [71, 72], ^{124}I-anti-PSCA (prostate stem cell antigen) A11 minibody for imaging of prostate cancer bone metastases [73] and ^{124}I-labeled purpurinimide derivative for tumor imaging [74], have been studied in a few subjects in each instance, ^{124}I-iodometomidate (^{124}I-IMTO) appears to be an attractive PET tracer for imaging adrenals [75].

Summary of clinical studies

Iodine-124 has now become established as a PET nuclide of considerable potential. Radioactive iodine itself has been a mainstay of Nuclear Medicine, and ^{124}I now brings the quantitative potential and superior contrast of PET to a wide variety of applications that have utilized other isotopes of iodine in the past. In particular, it has been found to be extremely useful in assessment of those patients in whom imaging is unsatisfactory with other radioisotopes. Figure 1 is an example of a patient with thyroid carcinoma (papillary at initial presentation) who had a negative ^{131}I scan; the pulmonary and cervical iodine-avid disease is clearly visualized in the ^{124}I PET scan, and serial imaging enabled calculation of tumor radiation dose from ^{131}I therapy.

Rapid clearance of radioiodine from the body is feasible with administration of stable iodide, and conjugating radioactive iodine to molecules of interest can thus be carried out with the secure knowledge that any radioactivity that becomes unbound will be rapidly eliminated, and with the knowledge that there is no non-specific accumulation in major organs like liver or bone marrow—an often vexing problem with radiometals. The relatively long half-life of ^{124}I lends itself to conjugation particularly with macromolecules that require imaging to be carried out days after administration of the radionuclide (a list of clinical trials utilizing ^{124}I PET is provided in the Table 1). Figure 2 is an example of a positive scan obtained a week after intravenous ^{124}I-girentuximab; the enhanced contrast is clearly evident. PET quantification has been found to be closely correlated with ex vivo measures of radioactivity

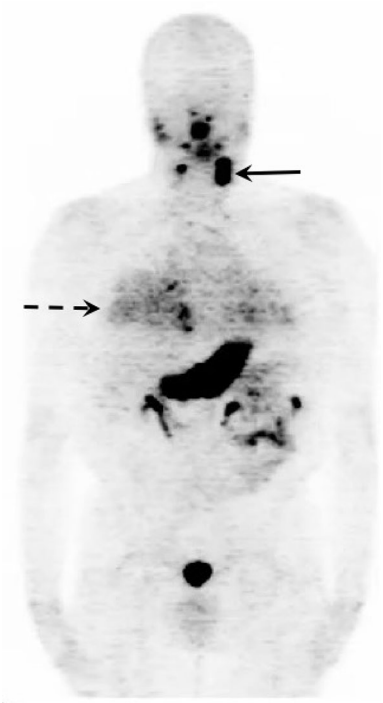

Fig. 1 3D Maximum intensity projection of a ^{124}I PET obtained 3 days after administration to a patient with papillary thyroid carcinoma (at presentation) who had a negative ^{131}I scan

concentration. Figure 3 is a digital autoradiograph from the resected clear cell renal carcinoma visualized in Fig. 2—the concordance between antigen expression (brown stain, right) with the distribution of radioactivity (dark, left) demonstrating the specificity of immunoPET.

Production and distribution of ^{124}I is certainly feasible with far fewer production sites than are necessary for shorter-lived nuclides; the relatively high (compared to 18F) whole body dose from ^{124}I remains a major drawback to its increasing use. So does its cost—this latter may however be considerably decreased if there is greater utilization (and thus demand) for ^{124}I. It is of course to be remembered that intracellular dehalogenation of radioiodine-conjugate molecules can occur, particularly when these are internalized through clathrin-coated pits. However, newer methods of conjugation may minimize/obviate this concern.

Exploration of the potential of PET using ^{124}I continues apace. Newer therapies in thyroid cancer are being explored with ^{124}I PET to assess and measure the feasibility of ^{131}I therapy. Conjugation of ^{124}I to a variety of molecules of varying sizes has enabled better assessment of disease, in particular the cancer phenotype. More accurate quantification also aids decision-making, be it for therapy with ^{131}I or for evaluation of therapeutic promise (a "predictive" biomarker) or efficacy (a "pharmacodynamic" biomarker). Crucial to the growth of ^{124}I PET will be a reduction in cost of production, potentially possible as more groups begin to produce this promising radionuclide.

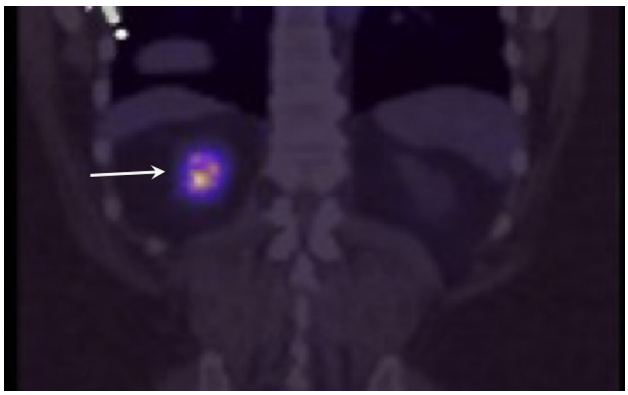

Fig. 2 Fusion coronal image of a PET/CT obtained a week after ^{124}I-girentuximab administration to a patient with clear cell renal cell carcinoma (ccRCC)

Table 1 Ongoing clinical trials: a list of current clinical trials that utilize ^{124}I-based PET/CT was obtained from the clinicaltrials.gov website. They include

S no.	Title	Identifier	Sponsor	Principal investigator
1	Phase I study to evaluate ^{124}I-A11 PSCA minibody in patients with metastatic prostate, bladder and pancreatic cancer	NCT02092948	Jonsson Comprehensive Cancer Center	Not provided
2	PET/CT imaging of malignant brain tumors with a novel radioiodinated phospholipid ether analogue ^{124}I-NM404	NCT01516905	University of Wisconsin, Madison	Lance Hall, MD Scott Perlman, MD, MS
3	^{124}I-Metaiodobenzylguanidine (MIBG) PET/CT diagnostic imaging and dosimetry for patients with neuroblastoma: A pilot study	NCT01583842	Katherine Matthay	Katherine Matthay, MD
4	The feasibility of novel ^{124}I-MIBG tracer in evaluation of myocardial sympathetic denervation and assessment of neuroendocrine tumors. Comparison with ^{123}I-MIBG	NCT01931488	Tel-Aviv Sourasky Medical Center	Einat Even Sapir, PhD, MD
5	Pilot trial to evaluate the utility of ^{124}I-cG250 for the early detection of response to therapy in patients with metastatic renal cell carcinoma	NCT01582204	Memorial Sloan Kettering Cancer Center	Steven Larson, MD
6	A cancer research UK phase I/II study to compare [^{124}I] Meta-Iodobenzylguanidine (mIBG) positron emission tomography/computerised tomography (PET/CT) to [^{123}I]mIBG imaging in patients with metastatic neuroblastoma	NCT02043899	Cancer Research UK	Sucheta Vaidya, Dr
7	A phase I study of convection-enhanced delivery of ^{124}I-8H9 for patients with non-progressive diffuse pontine gliomas previously treated with external beam radiation therapy	NCT01502917	Memorial Sloan Kettering Cancer Center	Mark Souweidane, MD
8	Clinical evaluation of a I-124 PET/CT based remnant radioiodine ablation decision concept in differentiated thyroid cancer using PROBE design	NCT01704586	University of Wuerzburg	Rainer Görges, MD, Ph.D. Peter F Schneider, MD, Prof.

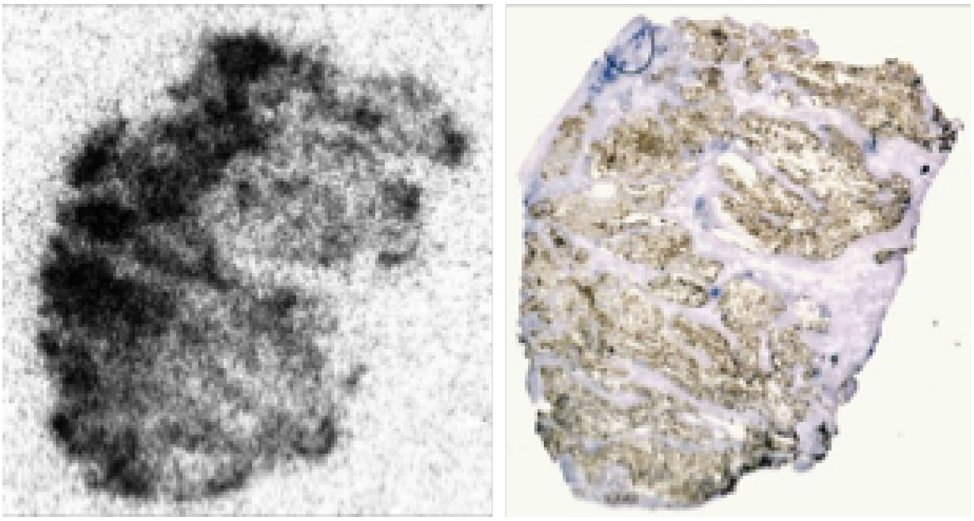

Fig. 3 Digital autoradiography (*left*) and immunohistochemistry (*right*) of the ccRCC obtained from patient in Fig. 2

Conclusion

This review summarizes the current and ongoing applications of ^{124}I as a PET radionuclide for molecular imaging. The positron emitting ability and 4.2 day half-life is particularly attractive for in vivo detection and quantification of slower biological and physiological processes.

Iodine-124 permits quantitative PET/CT of a wide variety of compounds, in addition to its use as the iodide in thyroid disorders. It is available throughout the world, although it currently is not inexpensive to produce. Its radiation dosimetry is similar to that of ^{131}I. Its half-life permits delayed images as well as autoradiography. Quantification of its distribution over time provides information regarding the biologic behavior of the agent to which it is attached, as well as enables estimates of radiation dose delivery (of therapeutic ^{131}I) that can be obtained with an accuracy comparable to ex vivo measurement. Pre-administration of stable iodide limits accumulation of radioiodine in normal tissue, reducing normal tissue toxicity.

Compliance with ethical standards

All procedures followed in the studies referenced were in accordance with the ethical standards of the responsible committee on human experimentation (institutional and national) and with the Helsinki Declaration of 1975, as revised in 2008. Informed consent was obtained from all patients for being included in the study.

Conflict of interest Dr. Sonia Mahajan reports no conflict of interest. Dr. Chaitanya Divgi reports no conflict of interest.

References

1. Delacroix D, Guerre JP, Leblanc P et al (2002) Radionuclide and radiation protection data handbook 2002. Radiat Prot Dosim 98(1):1–168
2. Pentlow KS, Graham MC, Lambrecht RM et al (1996) Quantitative imaging of iodine-124 with PET. J Nucl Med 37:1557–1562
3. Pentlow KS, Graham MC, Lambrecht RM et al (1991) Quantitative imaging of I-124 using positron emission tomography with applications to radioimmunodiagnosis and radioimmunotherapy. Med Phys 18:357–366
4. Belov VV, Bonab AA, Fischman AJ et al (2011) Iodine 124 as a label for pharmacological PET imaging. Mol Pharma 8:736–747
5. Koehler L, Gagnon K, McQuarrie S, Wuest F (2010) Iodine-124. A promising positron emitter for organic PET chemistry. Molecules 15:2686–2718
6. Braghirolli AM, Waissmann W, da Silva JB, dos Santos GR (2014) Production of iodine-124 and its applications in nuclear medicine. Appl Radiat Isot 90:138–148
7. Sajjad M, Bars E, Nabi HA (2006) Optimization of I-124 production via Te-124(p, n)I-124 reaction. Appl Radiat Isot 64:965–970
8. Nye JA, Avila-Rodriguez MA, Nickles RJ (2007) A new binary compound for the production of 124 I via the 124 Te (p, n) 124 I reaction. Appl Radiat Isot 65(4):407–412
9. Nagatsu K, Fukada M, Minegishi K et al (2011) Fully automated production of Iodine-124 using a vertical beam. Appl Radiat Isot 69:146–157
10. Aslam MN, Sudar S, Hussain M et al (2011) Evaluation of excitation functions of He-3 and alpha-particle induced reactions on antimony isotopes with special relevance to the production of iodine-124. Appl Radiat Isot 69:94–104
11. Uddin MS, Hermanne A, Sudar S et al (2011) Excitation functions of alpha particle induced reactions on enriched 123Sb and natSb for production of 124I. Appl Radiat Isot 69:699–704
12. Cascini GL, Asabella AN, Notaristefano A et al (2014) 124Iodine: a longer-life positron emitter isotope-new opportunities in molecular imaging. BioMed Res Int 2014:1–7
13. Bailey G (2002) The lactoperoxidase method for radiolabeling protein. In: Walker JM (ed) The protein protocols handbook. Humana Press, New York, pp 967–968
14. Chacko AM, Divgi CR (2011) Radiopharmaceutical chemistry with iodine-124: a non-standard radiohalogen for positron emission tomography. Med Chem 7:395–412
15. Eersels JLH, Travis MJ, Herscheid JDM (2005) Manufacturing I-123-labelled radiopharmaceuticals. Pitfalls and solutions. J Label Compd Radiopharm 48:241–257
16. Hunter DH, Zhu XZ (1999) Polymer supported radiopharmaceuticals: I-131 MIBG and I-123 MIBG. J Label Compd Radiopharm 42:653–661

17. Vaidyanathan G, Zalutsky MR (2007) Synthesis of N-succinimidyl 4-guanidinomethyl-3-[*I]iodobenzoate: a radio-iodination agent for labeling internalizing proteins and peptides. Nat Protoc 2:282–286
18. Darr AM, Opfermann T, Niksch T et al (2013) Low activity 124I-PET/low dose CT versus 99mTc-pertechnetate planar scintigraphy or 99mTc-pertechnetate single-photon emission computed tomography of the thyroid: a pilot comparison. Clin Nucl Med 38:770–777
19. Freudenberg LS, Antoch G, Jentzen W et al (2004) Value of 124I-PET/CT in staging of patients with differentiated thyroid cancer. Eur Radiol 14:2092–2098
20. Lubberink M, Abdul Fatah S, Brans B et al (2008) The role of 124I-PET in diagnosis and treatment of thyroid carcinoma. Q J Nucl Med Mol Imaging 52:30–36
21. Capoccetti F, Biggi E, Rossi G et al (2013) Differentiated thyroid carcinoma: diagnosis and dosimetry using 124I PET/CT. Clin Transl Imaging 1:185–193
22. Phan HT, Jager PL, Paans AM et al (2008) The diagnostic value of 124I-PET in patients with differentiated thyroid cancer. Eur J Nucl Med Mol Imaging 35:958–965
23. Freudenberg LS, Antoch G, Frilling A et al (2008) Combined metabolic and morphologic imaging in thyroid carcinoma patients with elevated serum thyroglobulin and negative cervical ultrasonography: role of 124I-PET/CT and FDG-PET. Eur J Nucl Med Mol Imaging 35:950–957
24. Capoccetti F, Criscuoli B, Rossi G et al (2009) The effectiveness of 124I PET/CT in patients with differentiated thyroid cancer. Q J Nucl Med Mol Imaging 53(5):536–545
25. Lubberink M, van Schie A, de Jong H et al (2006) Acquisition settings for PET of 124I administered simultaneously with therapeutic amounts of 131I. J Nucl Med 47:1375–1381
26. Beijst C, Kist JW, Elschot M et al (2016) Quantitative comparison of 124I PET/CT and 131I SPECT/CT detectability. J Nucl Med 57:103–108
27. Erdi YE, Macapinlac H, Larson SM et al (1999) Radiation dose assessment for I-131 therapy of thyroid cancer using I-124 PET imaging. Clin Positron Imaging 2:41–46
28. Eschmann SM, Reischel G, Bilger K et al (2002) Evaluation of dosimetry of radioiodine therapy in benign and malignant thyroid disorders by means of iodine-124 and PET. Eur J Nucl Med Mol Imaging 29:760–767
29. Pettinato C, Spezi E, Nanni C et al (2014) Pretherapeutic dosimetry in patients affected by metastatic thyroid cancer using 124I PET/CT sequential scans for 131I treatment planning. Clin Nucl Med 39:e367–e374
30. Jentzen W, Hoppenbrouwers J, van Leeuwen P et al (2014) Assessment of lesion response in the initial radioiodine treatment of differentiated thyroid cancer using 124I PET imaging. J Nucl Med 55:1759–1765
31. Jentzen W, Bockisch A, Ruhlmann M (2015) Assessment of simplified blood dose protocols for the estimation of the maximum tolerable activity in thyroid cancer patients undergoing radioiodine therapy using 124I. J Nucl Med 56:832–838
32. Jentzen W, Moldovan AS, Ruhlmann M et al (2015) Lowest effective 131I activity for thyroid remnant ablation of differentiated thyroid cancer patients. Dosimetry based model for estimation. Nuklearmedizin 54:137–143
33. Hartung-Knemeyer V, Nagarajah J, Jentzen W et al (2012) Pretherapeutic blood dosimetry in patients with differentiated thyroid carcinoma using 124-iodine: predicted blood doses correlate with changes in blood cell counts after radioiodine therapy and depend on modes of TSH stimulation and number of preceding radioiodine therapies. Ann Nucl Med 26:723–729
34. Ho AL, Grewal RK, Leboeuf R et al (2013) Selumetinib-enhanced radioiodine uptake in advanced thyroid cancer. N Engl J Med 368:623–632
35. Wierts R, Brans B, Havekes B et al (2016) Dose-response relationship in differentiated thyroid cancer patients undergoing radioiodine treatment assessed by means of 124I PET/CT. J Nucl Med (jnumed.115.168799) (Epub ahead of print)
36. Kist JW, de Keizer B, van der Vlies M et al (2015) 124I PET/CT to predict the outcome of blind 131I treatment in patients with biochemical recurrence of differentiated thyroid cancer; results of a multicenter diagnostic cohort study (THYROPET). J Nucl Med (jnumed.115.168799) (Epub ahead of print)
37. Khorjekar GR, Van Norstrand D, Garcia C et al (2014) Do negative 124I pretherapy positron emission tomography scans in patients with elevated serum thyroglobulin levels predict negative 131I posttherapy scans? Thyroid 24:1394–1399
38. Divgi CR, Pandit-Taskar N, Jungbluth AA et al (2007) Preoperative characterisation of clear-cell renal carcinoma using iodine-124-labelled antibody chimeric G250 (124I-cG250) and PET in patients with renal masses: a phase I trial. Lancet Oncol 8:304–310
39. Divgi CR, Uzzo R, Gatsonis C et al (2013) Positron emission tomography/computed tomography identification of clear cell renal cell carcinoma: results from the REDECT trial. J Clin Oncol 31:187–194
40. Pryma DA, O'Donoghue JA, Humm JL et al (2011) Correlation of in vivo and in vitro measures of carbonic anhydrase IX antigen expression in renal masses using antibody 124I-cG250. J Nucl Med 52:535–540
41. Carrasquillo JA, Pandit-Taskar N, O'Donoghue JA et al (2011) (124)I-huA33 antibody PET of colorectal cancer. J Nucl Med 52:1173–1180
42. O'Donoghue JA, Smith-Jones PM, Humm JL et al (2011) 124I-huA33 antibody uptake is driven by A33 antigen concentration in tissues from colorectal cancer patients imaged by immuno-PET. J Nucl Med 52:1878–1885
43. Schwartz J, Humm JL, Divgi CR et al (2012) Bone marrow dosimetry using 124I-PET. J Nucl Med 53:615–621
44. Jayson GC, Zweit J, Jackson A et al (2002) Molecular imaging and biological evaluation of HuMV833 anti-VEGF antibody: implications for trial design of antiangiogenic antibodies. J Natl Cancer Inst 94:1484–1493
45. Chacko AM, Li C, Nayak M et al (2014) Development of ^{124}I-Immuno-PET targeting tumor vascular TEM1/endosialin. J Nucl Med 55:500–507
46. Sharp SE, Trout AT, Weiss BD, Gelfand MJ (2016) MIBG in neuroblastoma diagnostic imaging and therapy. Radiographics 36:258–278
47. Hartung-Knemeyer V, Rosenbaum-Krumme S, Buchbender C et al (2012) Malignant pheochromocytoma imaging with 124I-mIBG PET/MR. J Clin Endocrinol Metab 97:3833–3834
48. Ezziddin S, Sabet A, Logvinski T et al (2013) Long-term outcome and toxicity after dose-intensified treatment with 131I-MIBG for advanced metastatic carcinoid tumors. J Nucl Med 54:2032–2038
49. Sharp SE, Shulkin BL, Gelfand MJ, Salisbury S, Furman WL et al (2009) 123I-MIBG scintigraphy and 18F-FDG PET in neuroblastoma. J Nucl Med 50:1237–1243
50. Sano Y, Okuyama C, Lehara T et al (2012) New semi-quantitative 123I-MIBG estimation method compared with scoring system in follow-up of advanced neuroblastoma: utility of total MIBG retention ratio versus scoring method. Ann Nucl Med 26:462–470
51. Yanik GA, Parisis MT, Shulkin BL et al (2013) Semiquantitative mIBG scoring as a prognostic indicator in patients with stage 4 neuroblastoma: a report from the Children's oncology group. J Nucl Med 54:541–548
52. Decarolis B, Schneider C, Hero B et al (2013) Iodine-123 metaiodobenzylguanidine scintigraphy scoring allows prediction of outcome in patients with stage 4 neuroblastoma: results of the Cologne interscore comparison study. J Clin Oncol 31:944–951

53. Cistaro A, Quartuccio N, Caobelli F et al (2015) I124-MIBG: a new promising positron-emitting radiopharmaceutical for the evaluation of neuroblastoma. Nucl Med Rev 18:102–106
54. Boellaard R, O'Doherty MJ, Weber WA et al (2010) FDG PET and PET/CT: EANM procedure guidelines for tumour PET imaging. Eur J Nucl Med Mol Imaging 37:1432–1433
55. Huang SY, Bolch WE, Lee C et al (2015) Patient-specific dosimetry using pretherapy [^{124}I]m-iodobenzylguanidine ([^{124}I]mIBG) dynamic PET/CT imaging before [^{131}I]mIBG targeted radionuclide therapy for neuroblastoma. Mol Imaging Biol 17:284–294
56. Rischin D, Hicks RJ, Fisher R et al (2006) Prognostic significance of [18F]-misonidazole positron emission tomography-detected tumor hypoxia in patients with advanced head and neck cancer randomly assigned to chemoradiation with or without tirapazamine: a substudy of Trans-Tasman Radiation Oncology Group Study 98.02. J Clin Oncol 24:2098–2104
57. Rajendran JG, Krohn KA (2015) F-18 fluoromisonidazole for imaging tumor hypoxia: imaging the microenvironment for personalized cancer therapy. Semin Nucl Med 45:151–162
58. Okamoto S, Shiga T, Yasuda K et al (2013) High reproducibility of tumor hypoxia evaluated by 18F-fluoromisonidazole PET for head and neck cancer. J Nucl Med 54:201–207
59. Reischl G, Dorow DS, Cullinane C et al (2007) Imaging of tumor hypoxia with [124I]IAZA in comparison with [18F]FMISO and [18F]FAZA–first small animal PET results. J Pharm Pharm Sci 10:203–211
60. Wang Z, Hong X, Zong S et al (2015) BODIPY-doped silica nanoparticles with reduced dye leakage and enhanced singlet oxygen generation. Sci Rep 5:12602
61. Lee J, Lee TS, Ryu J et al (2013) RGD peptide-conjugated multimodal NaGdF4:Yb3+/Er3+nanophosphors for upconversion luminescence, MR, and PET imaging of tumor angiogenesis. J Nucl Med 54:96–103
62. Simone EA, Zern BJ, Chacko AM et al (2012) Endothelial targeting of polymeric nanoparticles stably labeled with the PET imaging radioisotope iodine-124. Biomaterials 33:5406–5413
63. Pandey S, Venugopal A, Kant R et al (2014) 124I-Epidepride: a PET radiotracer for extended imaging of dopamine D2/D3 receptors. Nucl Med Biol 41:426–431
64. Zechmann C, Oromieh AA, Armor T et al (2014) Radiation dosimetry and first therapy results with a I124/I131 labeled small molecule (MIP-1095) targeting PSMA for prostate cancer therapy. Eur J Nucl Med Mol Imaging 41:1280–1292
65. Koehler L, Graf F, Bergann R et al (2010) Radiosynthesis and radiopharmacological evaluation of cyclin-dependent kinase 4 (Cdk4) inhibitors. Eur J Med Chem 45:727–737
66. Stahlschmidt A, Machulla HJ, Reischl G et al (2008) Radioiodination of 1-(2-deoxy-beta-D-ribofuranosyl)-2,4-difluoro-5-iodobenzene (dRFIB), a putative thymidine mimic nucleoside for cell proliferation studies. Appl Radiat Isot 66:1221–1228
67. Williams H, Julyan P, Ranson M et al (2007) Does 124Iododeoxyuridine measure cell proliferation in NSCLC? Initial investigations with PET imaging and radio-metabolite analysis. Eur J Nucl Med Mol Imaging 34:301–303
68. Roelcke U, HausmannO Merlo A et al (2002) PET imaging drug distribution after intratumoral injection: the case for (124)I-iododeoxyuridine in malignant gliomas. J Nucl Med 32:1444–1451
69. Wang HE, Yu HM, Liu RS et al (2006) Molecular imaging with 123I-FIAU, 18F-FUdR, 18F-FET, and 18F-FDG for monitoring herpes simplex virus type 1 thymidine kinase and ganciclovir prodrug activation gene therapy of cancer. J Nucl Med 47:1161–1171
70. Pal A, Glekas A, Doubrovin M et al (2006) Molecular imaging of EGFR kinase activity in tumors with 124I-labeled small molecular tracer and positron emission tomography. Mol Imaging Biol 8:262–277
71. Glaser M, Collingridge DR, Aboagye EO et al (2003) Iodine-124 labelled annexin-V as a potential radiotracer to study apoptosis using positron emission tomography. Appl Radiat Isot 58:55–62
72. Dekker B, Keen H, Lyons S et al (2005) MBP-annexin V radiolabeled directly with iodine-124 can be used to image apoptosis in vivo using PET. Nucl Med Biol 32:241–252
73. Knowles SM, Tavare R, Zettlitz KA et al (2014) Applications of immunoPET: using 124I-anti-PSCA A11 minibody for imaging disease progression and response to therapy in mouse xenograft models of prostate cancer. Clin Cancer Res 20:6367–6378
74. Pandey SK, Sajjad M, Chen Y et al (2009) Compared to purpurinimides, the pyropheophorbide containing an iodobenzyl group showed enhanced PDT efficacy and tumor imaging (124I-PET) ability. Bioconjug Chem 20:274–282
75. Kvaternik H, Wanek T, Hammerschmidt F et al (2014) Radiosynthesis of 124I-iodometomidate and biological evaluation using small-animal PET. Mol Imaging Biol 16:317–321